ELSEVIER

Biophysical Chemistry 101–102 (2002) 447–459

Biophysical Chemistry

www.elsevier.com/locate/bpc

Wall effects on DNA stretch and relaxation☆

Dirk Stigter*

Department of Pharmaceutical Chemistry, University of California, San Francisco, CA 94143, USA

Received 19 November 2001; accepted 5 December 2001

Abstract

Hydrodynamic wall effects are treated with an image or reflection method. This method uses a mirror image of the molecule, with the opposite velocity, to satisfy the non-slip boundary condition of zero velocity of the liquid at the wall. Molecules moving inside a slit require an infinite series of images, or reflections from both walls, whose effects converge slower for thinner slits. It is shown that, with the same external field, wall effects increase the electrophoretic stretch of DNA, more so for thinner slits. The theory is in fairly good agreement with stretch experiments on T4 DNA in slits of width 5, 0.3, and 0.09 μm by Bakajin et al. (Phys. Rev. Let. 80 (1998) 2737). For the same slits relaxation data are available for T4 DNA first hooked around an obstacle, stretched in a U-shape in an external electric field, and sliding off until the stretched molecule moves away in free electrophoresis. The theory approximates the relaxation of the molecule, after detachment from the obstacle, as the relaxation of tethered DNA stretched in a temporary electric field. The theory agrees fairly well with the experiments. The significance of electroosmotic flow is discussed for electrophoretic experiments. An Appendix gives numerical data on the free electrophoresis of unstained and stained DNA, and discusses problems of the kinetic diameter of DNA.

Keywords: Hydrodynamic interaction; Entropic elasticity; Fluctuations; Electrophoretic stretch; Free solution electrophoresis of DNA; Stained DNA; Kinetic diameter of DNA

1. Introduction

In recent years theories have been developed for the electrophoretic stretch and relaxation of tethered DNA in free solution and in agarose gels [1,2]. In this paper we treat the effects of nearby cell walls. The object is to interpret the results of Bakajin et al. [3] who measured the electrophoretic stretch and relaxation of single T4 DNA molecules in buffer solutions confined to thin slits. Walls may modify the elastic and the hydrodynamic properties of DNA. We apply a reflection method [4] to approximately satisfy the hydrodynamic non-slip boundary condition at the walls of the slit. As before, the relevant differential equations would be difficult to solve analytically. Therefore, the problems are formulated in terms of difference equations which are solved numerically. In the

☆ I dedicate this paper to John Schellman with deep appreciation for his sound scientific advice during many years of friendship.

*1925 Marin Avenue, Berkeley, CA 94707-2407, USA. Tel.: +1-510-526-4989.

E-mail address: stigter@maxwell.ucsf.edu (D. Stigter).

0301-4622/02/$ - see front matter © 2002 Elsevier Science B.V. All rights reserved.
PII: S0301-4622(02)00166-7

next section we first review various aspects of the DNA model.

2. Model of DNA

2.1. Hydrodynamics

We use the model introduced by Stigter and Bustamante [1] and developed pictorially in Fig. 1. The traditional pearl necklace polymer model of Fig. 1a is well chosen for treating the long-range hydrodynamic interactions between remote sections of the polymer, but it is unsuitable for dealing with the much shorter range, steeper liquid velocity gradients around a polyelectrolyte chain in electrophoresis. For the latter purpose we use the freely jointed chain model in Fig. 1b, the segmented chain with N cylindrical Kuhn segments of length $2P$ where P is the persistence length of the chain. The hydrodynamics of short cylinders, however, is not known with any accuracy. For this reason the cylindrical segments are recast as prolate ellipsoids of the same length and volume. The friction coefficient of such ellipsoids is known as a function of size and orientation [5]. The flow field around a moving ellipsoid is not available in closed form, but requires about half a page of computer code for exact evaluation. Fortunately, this flow field can be well approximated by that around a solid sphere with the same friction coefficient as the ellipsoid [2]. For hydrodynamic purposes, therefore, we represent each cylindrical chain segment i in Fig. 1b by an equivalent sphere with a radius a_i that reflects the size of the segment and its orientation, compare Fig. 1c–e

$$a_i = a_{\parallel}\cos^2\theta_i + a_{\perp}\sin^2\theta_i \quad (1)$$

where θ_i is the angle between the long axis of the segment and the direction of its motion along the z-axis. We assume the earlier value [2] $2P = 1300$ Å for the length of a stained DNA segment and, following Eimer and Pecora [6], we take 20 Å for the hydrodynamic diameter of B-DNA. This gives [1] $a_{\parallel} = 104.0$ Å and $a_{\perp} = 167.8$ Å.

The pearl necklace model of stained DNA with a contour length of $1300N$ Å has $65N$ spheres. We now treat the hydrodynamics of the same DNA with a constellation of N spheres. Compared with the pearl necklace model this reduces the pair interactions by a factor $65^2 = 4225$, without significant loss of accuracy. In his treatment of hydrodynamic stretch of DNA Zimm [7] defines hydrodynamic chain segments in a different way, but with the same purpose of reducing the number of pair interactions.

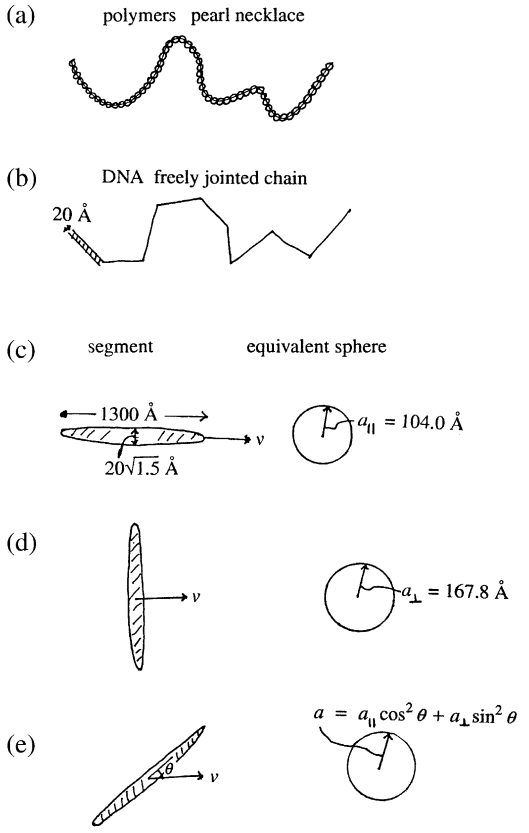

Fig. 1. Models of DNA: (b) for electrophoresis and chain statistics. (c)–(e) For hydrodynamics of segments of stained DNA. See text.

2.2. Electrophoresis

We use the freely jointed chain model of Fig. 1b. The electrophoretic motion of an isolated, cylindrical chain segment is in the direction z of the applied field E only for parallel or transverse orientation. In general, when the isolated segment i makes an angle θ_i with the field E, the segment does not move in the direction of E. Here we need

the projection of the electrophoretic velocity of segment i on the z-axis [1]

$$v_i^{el} = \frac{\varepsilon_0 D\zeta E}{\eta}\left(\cos^2\theta_i + \frac{2}{3}g_\perp \sin^2\theta_i\right) \quad (2)$$

where ζ is the surface potential of the stained B-DNA in the solution with viscosity η and dielectric constant D, ε_0 is the permittivity of free space, and $g_\perp$ is a numerical factor for the cylindrical segment in transverse electrophoresis [8]. Since the electrophoretic flow field is very short range [2], we shall ignore wall effects in Eq. (2) and on the electrophoretic force on a single segment in Eq. (10) below. Numerical details for the free solution electrophoresis of DNA are given in Appendix A.

2.3. Elasticity of DNA

When a DNA chain is stretched by pulling the ends apart, it can access fewer conformations than in the unstretched state. This difference gives rise to an entropic elasticity. We use the theory of Marko and Siggia [9] for the entropic elasticity of wormlike chains under constant tension. The results, as given by Zimm [7], are applied to single Kuhn segments of contour length $2P$. When the extension of a segment i under tension T_i is $z_i = 2P\langle\cos\theta_i\rangle$, the orientation of the segment is given by

$$\frac{z_i}{2P} = \langle\cos\theta_i\rangle = \frac{0.6667t + 0.8080t^2 + 0.10365t^3}{1 + 1.1118t + 1.1076t^2 + 0.10365t^3} \qquad t \leqslant 9 \quad (3a)$$

$$\langle\cos\theta_i\rangle = 1 - \frac{0.5}{t^{1/2}} \quad t > 9 \quad (3b)$$

In Eqs. (3a) and (3b) t is the dimensionless reduced tension

$$t = \frac{T_i P}{k_B T} \quad (4)$$

where $k_B T$ is Boltzmann's constant times the absolute temperature.

In Eqs. (1) and (2), and in other relations below, we need the average square value, $\langle\cos^2\theta_i\rangle$, instead of the average value, $\langle\cos\theta_i\rangle$, from Eqs. (3a) and (3b). In Refs. [1] and [2] we have used $\langle\cos^2\theta_i\rangle = \langle\cos\theta_i\rangle^2$, shown to be a good approximation for the hydrodynamic stretch of freely jointed chains [1]. At present we use for $\langle\cos^2\theta_i\rangle$ a more satisfactory expression derived from fluctuation theory [10]

$$\langle\cos^2\theta_i\rangle = \langle\cos\theta_i\rangle^2 + \frac{1}{2}\left(\frac{\partial\langle\cos\theta_i\rangle}{\partial t}\right)_{T,P} \quad (5)$$

where Eqs. (3a) and (3b) is now used also for the derivative term in Eq. (5). Zimm [7] has used an equivalent of Eq. (5) to describe the observed density distribution of the chain image in hydrodynamic stretch. More recently Bouchiat et al. [11] have derived a ten term expression for T_i as a function of $\cos\theta_i$, the inverse of Eqs. (3a) and (3b), which in Eq. (5) is less convenient to use than Eqs. (3a) and (3b). The accuracy of Eqs. (3a) and (3b) is of the order of 1%, sufficient for present purposes.

Eqs. (3a) and (3b) has been derived for a chain stretched in bulk solvent, unhindered by any walls. Is this elasticity changed when the chain is confined in a slit? We consider a polymer chain inside a slit with walls at $y = 0$ and $y = w$. The chain is stretched parallel to the walls, in the z direction. Chain statistics are often based on the assumption that the statistics in the x, y, and z directions are independent of each other. For example, for a Gaussian distribution the probability $W(r)$ of finding the end-to-end distance r of a randomly coiled polymer is the product of three factors that depend, respectively, on the components x, y, and z of r

$$W(r) = X(x)Y(y)Z(z) \quad (6)$$

Confinement of the chain in the slit affects the $Y(y)$ factor of $W(r)$, but the elasticity of the stretched chain depends on $Z(z)$. So, to the extent that Eq. (6) is valid, the chain elasticity does not depend on the slit width w. This cannot be generally true. The condition $x^2 + y^2 + z^2 = r^2$ restricts the independence of x, y, and z in Eq. (6). Furthermore, when the slit width w becomes small compared to the persistence length P of the chain, we go from three-dimensional to two-dimensional chain statistics, with a longer end-to-end distance

[12]. Incorporating wall effects in the Marko–Siggia theory [9] is beyond the scope of this paper. We shall use Eqs. (3a) and (3b) without corrections.

2.4. Chain statistics

As before [1,2], we use the freely jointed chain model, dividing the chain into N Kuhn segments with segment $k=1$ tethered and segment $k=N$ at the free end of the chain. The chain is stretched in the z direction, and Eqs. (3a) and (3b) is applied to each segment k to find the (average) cosine of the angle θ_k with the z-axis from the tension T_k in the segment. The angle ϕ_k between the x-axis and the projection of segment k on the xy-plane completes the orientation of the segment. In the earlier work [1,2] all angles ϕ_k were chosen randomly, beginning with the tethered segment $k=1$. Here we proceed in the same way, knowing that the beginning of segment 1, at the tether point, is inside the slit. After a random choice of ϕ_1 between 0 and 2π we test whether the segment is completely inside the slit. If not, ϕ_1 is divided by 2 and the segment is tested again, etc. The angle ϕ_1 is halved until the projection of the segment on the y-axis, $2P \sin\theta_1 \sin\phi_1$, is small enough to keep the segment fully inside the slit. In the same way each succeeding segment is also confined inside the slit.

In electrophoretic stretch calculations Eq. (5) allows the inclusion of fluctuations in the chain extension. Instead of using the average extension, $\mathrm{Ex}=2P\sum_{i=1}^{N}\langle\cos\theta_i\rangle$, we now add the r.m.s. fluctuations

$$\mathrm{Ex}=2P\sum_{i=1}^{N}\langle\cos\theta_i\rangle+P\left[\sum_{i=1}^{N}\left(\frac{\partial\langle\cos\theta_i\rangle}{\partial t}\right)_{T,P}\right]^{1/2} \qquad (7)$$

Fig. 2 shows the difference for a chain of stained DNA with $N=200$ segments in $0.5\times$TBE buffer. The changes are minor, except at low extensions where Ex does not vanish any longer, but now extrapolates to a finite value, as found in the early experiments by Smith and Bendich [13].

For the average values from Eqs. (3a), (3b) and (5), we shall omit the brackets in the text below.

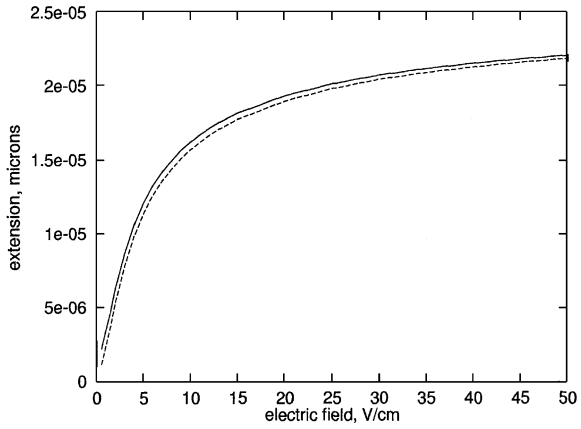

Fig. 2. Electrophoretic stretch of stained DNA with $N=200$ segments versus external electric field. *Solid curve:* with fluctuations from Eq. (7). *Dashed curve:* without fluctuations.

3. Electrophoretic stretch of DNA in thin slits

With the foregoing model we now consider the DNA chain consisting of $k=1$ to N Kuhn segments, tethered in solution at the $k=1$ end, and stretched by an external electric field E in the z direction. The tension T_k in segment k is assumed to be uniform and equal to the sum of the electrophoretic forces F_i on segments $i=k+1$ to N, on the free end of the chain

$$T_k=\sum_{i=k+1}^{N}F_i \qquad (8)$$

with

$$F_i=F_i^0+6\pi\eta a_i\sum_{j=1}^{N}\Delta u_{ij}^0 \qquad j\neq i \qquad (9)$$

F_i^0 is the electrophoretic force on the single segment i given by [1]

$$F_i^0=\frac{\varepsilon_0 D\zeta E}{\eta}\times(6\pi\eta a_{\parallel}\cos^2\theta_i+4\pi\eta a_{\perp}g_{\perp}\sin^2\theta_i) \qquad (10)$$

The sum of terms in Eq. (9) is due to the hydrodynamic interaction of segment i with all the other segments, j, of the chain, as caused by the electric force on the countercharge in the solution around the DNA. In an unrestricted solution the flow perturbation of segment j is [1]

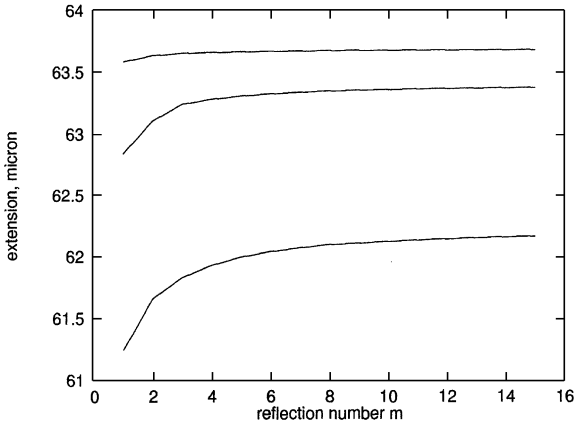

Fig. 3. Electrophoretic extension of T4 DNA versus reflection number m in Eq. (12) in different slits and different fields. *From top to bottom:* $w=5$ μm, $E=40$ V cm^{-1}; $w=0.3$ μm, $E=17$ V cm^{-1}; $w=0.09$ μm, $E=9$ V cm^{-1}.

$$\Delta u_{ij}^0 = u_j\left[\left(-\frac{3}{4}\frac{a_j}{r_{ij}}-\frac{1}{4}\frac{a_j^3}{r_{ij}^3}\right) -\cos^2\theta_{ij}\left(\frac{3}{4}\frac{a_j}{r_{ij}}-\frac{3}{4}\frac{a_j^3}{r_{ij}^3}\right)\right] \quad j\neq i \tag{11}$$

In Eq. (11) $u_j=F_j/6\pi\eta a_j$ is the local liquid velocity at segment j, r_{ij} is the distance between segments i and j with the condition $r_{ij}\geqslant a_i+a_j$, and θ_{ij} is the angle between the distance vector r_{ij} and the z-axis. The expression in square brackets is the relative magnitude in the z direction at segment i of the flow originating at segment j.

For the effect of a single wall on the hydrodynamics, we use the image or reflection method which is well established in fluid dynamics [4], and has been employed e.g. by Zimm [7]. To satisfy the condition of zero liquid velocity at the wall, located at $y=0$, it is a good approximation to replace the wall by the mirror image of the chain with the same velocity in the opposite direction. When the real molecule has segments at (x_j, y_j, z_j), its image has segments at $(x_j, -y_j, z_j)$. Reflection means that in Eq. (9) we subtract a second interaction term proportional to a sum $\sum_{j=1}^{N}\Delta u_{ij}(-y_j)$. This sum is similar to that in Eq. (9), but in Eq. (11) r_{ij} now refers to the distances between segment i in the real chain and segment j in its image, and $j=i$ is included.

Extending to a molecule in a slit, we have multiple reflections from both walls, with the flow changing sign at each reflection. With parallel walls at $y=0$ and $y=w$ a segment j at y_j inside the slit has an infinite series of images, at $-y_j$ and at $2mw-y_j$, $-2mw-y_j$, $2mw+y_j$, and $-2mw+y_j$, with $m=1$ to ∞. Each of the $1+4m$ images of the molecule contributes to the electrophoretic force F_i terms as in Eq. (11), where in Eq. (9) the sum is subtracted for an odd number of reflections, and added for an even number of reflections

$$F_i = F_i^0 + 6\pi\eta a_i\sum_{j=1}^{N}\Big\{\Delta u_{ij}^0-\Delta u_{ij}(-y_j) + \sum_{m=1}^{\infty}\big[-\Delta u_{ij}(2mw-y_j)-\Delta u_{ij}(-2mw-y_j) +\Delta u_{ij}(2mw+y_j)+\Delta u_{ij}(-2mw+y_j)\big]\Big\} \tag{12}$$

Eq. (12) contains a series in m whose convergence depends on the ratio w/a_i. Fig. 3 shows the electrophoretic stretch of a 74 μm long DNA molecule tethered in three different slits, calculated as a function of m. The results show that, from top to bottom, the series in Eq. (12) converges slower for narrower slits.

Eqs. (8)–(12) give the tensions in the segments and Eqs. (3a) and (3b) the corresponding segment extensions. As explained in Ref. [1], an iterative computation produces sets of selfconsistent values for T_k and $\cos\theta k$, and with Eq. (7) the chain extension.

4. Relaxation of DNA stretched in thin slits

The relaxation of deformed DNA in solution to form a random coil is driven by its entropic elasticity. We treat the relaxation dynamics of stretched DNA as a mechanical equilibrium between elastic forces contracting the chain and friction forces of the chain with the solvent opposing such contraction, beginning with ideas used already in Ref. [2]. In the experiments of Bakajin et al. [3] single DNA molecules, first hooked

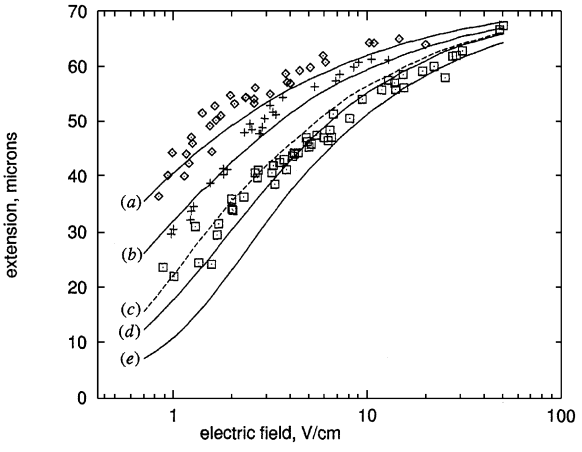

Fig. 4. Electrophoretic extension of T4 DNA versus external electric field in slits of width $w=0.09$ μm (curve *a*, diamonds); $w=0.3$ μm (curve *b*, crosses); $w=5$ μm (curves *c*, *d*, and *e*, squares). Solid curves for same random number sequence. Curves *a*, *b*, and *e* tethered in center plane of slit, *c* and *d* at 0.1 μm from wall. Points from experiments by Bakajin et al. [3].

around a post and stretched in a U-shape by the external electric field, were allowed to slide off the post. Contraction, or relaxation, of the stretched molecule was observed starting immediately after detachment from the post. The relaxation was found to be slower in thinner slits. To fit the experimental conditions above, the earlier relaxation theory [2] needs to be extended in two ways. First, the relaxing molecule is not tethered as in Ref. [2], but free floating in the applied electric field, and, second, wall effects are significant. As in Ref. [2] the relaxation is driven by elastic tension gradients. So the treatment should start with the tension distribution along the stretched, just detached molecule. At present there are no suitable experiments or theory that yield the desired tension distribution. We first review the relaxation of free floating chains, and then show how relevant experiments lead to some useful approximations.

In the tethered chain of Ref. [2] the tension, T_k in segment k, increases from the free end, $T_N=0$ in segment N, to a maximum, T_1 in the tethered segment $k=1$. During relaxation of the chain the shortening of segment k is driven by the tension difference $\Delta T_k=T_k-T_{k+1}$. This difference is compensated by the friction force on the free end of the chain, on segments $i=k+1$ to $i=N$, all moving with the velocity v_k that shortens segment k,

$$\Delta T_k=v_k\sum_{i=k+1}^{N} f_i \tag{13}$$

where $v_k f_i$ is the friction force on segment i. For the free floating chain we assume that the relaxation is not coupled to the electrophoresis of the chain, that is, electrophoretic motion does not change the elastic tension in the molecule. The elastic tension vanishes at both ends of the chain and, hence, it must be maximal, T_m in a segment m, at some distance from the ends. In the leading part of the chain, from $k=m$ to N, the relaxation is the same as above, as if the chain were tethered at segment m without external electric field. In the trailing part of the chain the sign of the relaxation process is reversed. Here the relaxation velocity of segment k for $k=1$ to $k=m-1$ is $v_k=(T_k-T_{k-1})/\sum_{i=1}^{k-1} f_i$, where f_i is the friction coefficient of segment i in the trailing free end of the chain, segments 1 to $k-1$. In summary, the free floating chain relaxes from both ends toward the point of maximum tension in segment m. We approximate the position of segment m on the basis of two experimental observations.

Gurrieri et al. [14] have published a series of pictures of the unhooking and subsequent relaxation of a stained 1.6 Mbp DNA molecule in an agarose gel. The pictures show that relaxation of the stretched molecule into a random coil is evident only at the leading end, but not at all at the trailing end. This suggests that in the detaching molecule the tension peaks relatively close to the trailing end, so that relaxation from the leading end dominates and relaxation from the trailing end is negligible. A paper by Song and Maestre [15] on the unhooking dynamics provides supporting evidence. Measurements on U-shaped DNA during gel electrophoresis show that the extension of five molecules during unhooking varied on average less than 15%. As in Ref. [14] a small amount of relaxation was evident in the later stages of unhooking. This may show that electrophoretic stretch is the major factor in determining the

molecular extension during unhooking. On this basis we approximate the tension distribution at the end of the unhooking process as if it were determined purely by electrophoretic stretch of a tethered molecule. In our model we assume $m=1$ and we treat the relaxation of the detaching molecule, moving in free electrophoresis, as if it remains tethered at segment 1 with the external field turned off. With this approximation we now introduce wall effects.

The relaxation treatment in Ref. [2] is for DNA relaxing in an infinite amount of solution. In Eq. (27) of Ref. [2] the segmental friction forces are given for chain relaxation in a gel. In the present case of relaxation in a slit we have, in view of Eqs. (11) and (12), for the friction force on a segment i in the free end of the chain

$$\upsilon_k f_i = 6\pi\eta a_i \upsilon_k + 6\pi\eta a_i \sum_{j=k+1}^{N} \times \left\{ \Delta u_{ij}^0 - \Delta u_{ij}(-y_j) + \sum_{m=1}^{\infty} \left[-\Delta u_{ij}(2mw - y_j) - \Delta u_{ij}(-2mw - y_j) + \Delta u_{ij}(2mw + y_j) + \Delta u_{ij}(-2mw + y_j) \right] \right\} \quad (14)$$

with in Eq. (11) the local liquid velocity at segment j now given by $u_j = \upsilon_k f_j / 6\pi\eta a_j$. As in Ref. [2] we keep the velocities υ_k constant over short time intervals Δt. The fully relaxed free end of the chain is treated as a random coil. Chain extensions are obtained by adding segment extensions. Plotting these versus the relevant sum of time intervals gives the relaxation curve.

5. Comparison with experiments

In this section we consider the experiments of Bakajin et al. [3] who measured the electrophoretic stretch and the relaxation of single DNA molecules in thin slits filled with Tris–Borate–EDTA buffer (0.5×TBE). Observations of electrophoretic stretch were on T4 DNA (167 kbp) stained with TOTO-1 dye, hooked symmetrically over a post between the cell walls. Staining of the DNA added approximately 30% to the contour length of the molecules which were found to be approximately 74 μm long. As in Refs. [2] and [3] we assume that staining increased the persistence length of the DNA also by 30%.

5.1. Electrophoretic stretch

Fig. 4 is a modified copy of Fig. 2 of Bakajin et al. [3] showing the extension of the DNA stretched in fields of approximately $E=1$ to 50 V cm^{-1} in three different slits. In Ref. [3] the extensions are plotted versus a flow velocity $\upsilon = u_{\mathrm{av}}E$, where u_{av} is the electrophoretic mobility of coiled DNA as measured in an obstacle-free part of the solution. The value of u_{av}, however, is not reported in Ref. [3], causing some uncertainty in the data. The points in Fig. 2 of Ref. [3] cover the range of $\upsilon = 2.14$ to 128 μm s^{-1}, somewhat larger than the 50-fold range, 1 to 50 V cm^{-1}, reported for E. To make progress we have assumed that the highest field used was $E=50$ V cm^{-1}. The resulting mobility of coiled DNA, $u_{\mathrm{av}} = 128$ μm s^{-1}/50 V cm^{-1} $= 2.56\times10^{-4}$ cm^2 V^{-1} s^{-1}, gives $e\zeta/kT = -2.01$ and $g_\perp = 0.684$, see Appendix A, Table 2. With this information we have used Eqs. (3a), (3b), (7), (8) and (12) above with the numerical iteration method of Ref. [1], and obtained the curves in Fig. 4.

From top to bottom the curves in Fig. 4 are for increasing width w of the cell. The two top curves, marked *a* and *b*, are fairly close to the experiments for $w=0.09$ and 0.3 μm The three lower curves are for $w=5$ μm, calculated for different conditions. For narrow slits the DNA chain is frequently in contact with one of the walls, fixing the y-position of the chain within narrow limits. Therefore, the stretch curve is not very sensitive to the assumed tether position of the chain on the post, or to the random sequence used for the chain conformations. This is different for relatively wide slits such as for $w=5$ μm. The lowest curve, *e*, in Fig. 4 is for DNA tethered in the center plane of the cell, as in curves *a* and *b*. Curves *c* and *d* are for DNA tethered close to a wall, at $y(1)=0.1$ μm, compared with $y(1)=2.5$ μm for curve *e*. We find that the difference is quite significant. For curves *c* and *d* the chain approaches the wall at $y=0$ much closer than for curve *e* and, hence, the first hydrodynamic reflection increases the friction

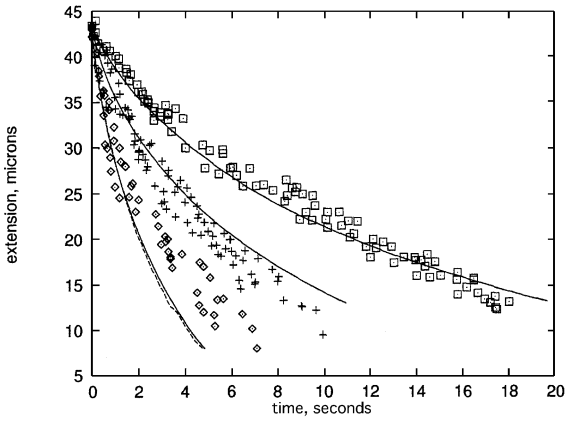

Fig. 5. Relaxation of stretched T4 DNA in slits of different widths. *From left to right:* slit width $w=5$, 0.3, 0.09 μm. Points from experiments by Bakajin et al. [3].

of the chain much more. All solid curves are for the same random sequence for the conformations, but for the dashed curve a different random sequence was chosen, leading to a significant difference between curves *c* and *d*. From the differences between curves *c*, *d*, and *e* we anticipate that, if we evaluate stretch curves for various tether points across the slit and for various random sequences, the average stretch curve for $w=5$ μm would agree reasonably well with the experimental points. The uncertainty of the electrophoretic mobility and, hence, the ζ potential of DNA, and the possible significance of electroosmotic flow (see below) might also influence the fit between theory and experiment in Fig. 4.

5.2. Relaxation

In Ref. [3] U-shaped DNA molecules were stretched in the three different slits by electric fields that were adjusted to give an extension of approximately 44 μm at detachment. The experimental extension-time observations of the subsequent relaxation are shown in Fig. 5. For the T4 DNA molecules, with a contour length of approximately 74 μm [3], relaxation calculations with $N=563$ segments for the tethered molecule require very long computer times. This is so in particular for narrow slits, where many reflections are needed in Eq. (14) with every update of the friction coefficients. Therefore, we have used relaxation of shorter molecules and scaling to obtain the relaxation curves for T4 DNA.

As pointed out in [2], scaling is not perfect because a plot of log(Ex) versus time t is not quite linear. So the exponent α in the scaling equation $\mathrm{Ex}=t/N^{\alpha}$ depends on the range of the relative chain extension Ex selected to evaluate α. We have used $\mathrm{Ex}=0.6$ and 0.1, and $N=100$ and 200, to find the exponents for the three different slits: $\alpha=1.465$ for slit width $w=5$ μm, $\alpha=1.655$ for $w=0.3$ μm, and $\alpha=1.790$ for $w=0.09$ μm. The relaxation for $N=563$, extrapolated from the $N=200$ results by scaling, is shown in Fig. 5 as solid curves for the three slits. In the widest slit, $w=5$ μm, relaxation was also computed directly for $N=563$. The results, shown as the dashed curve in Fig. 5, are very close to the relevant solid curve, evidence of the good quality of the scaled curves.

The computations assume that the molecules are tethered in the center of the slits. As in Fig. 4 above, this might not correspond to the experiments. If the relaxing molecule was off center and close to a wall, its friction factor increased and its relaxation was slower than calculated. This effect would be most significant in the wide slit, with $w=5$ μm, and might explain why the theoretical relaxation is significantly faster than the experiments in this slit. In view of the various approximations and uncertainties the agreement between theory and experiment is satisfactory.

6. Discussion

As shown in Table 2 of the Appendix A, in 0.5×TBE buffer solution the smallest estimate of the surface potential of DNA, stained with TOTO-1, is $e\zeta/kT=-1.98$. The potential estimated from the measurements of Bakajin et al. [3], $e\zeta/kT=-2.01$, is nearly the same. This close agreement might be accidental, see Appendix A, and does not rule out electroosmotic flow. Without presenting evidence, Bakajin et al. [3] state that 'Electroosmotic flow, induced by surface charges, was negligible.'

In general, the most effective way to prevent electroosmosis in electrophoretic experiments is

Table 1
Electrophoresis of DNA in solutions of KCl $N(CH_3)_4Cl$ (TMACl), Tris–Acetate (TA)

α	y_0	$u_\parallel$	$u_\perp$		
			KCl	TMACl	TA
$C_{salt}=0.003$ M					
0.05	0.81	1.62	0.81	0.81	0.81
0.10	1.59	3.18	1.54	1.52	1.50
0.15	2.31	4.61	2.12	2.09	2.04
0.20	2.95	5.90	2.57	2.51	2.41
0.25	3.52	7.03	2.90	2.81	2.66
0.30	4.01	8.02	3.14	3.01	2.83
0.35	4.44	8.87	3.31	3.16	2.94
0.40	4.81	9.62	3.44	3.26	3.02
0.45	5.14	10.28	3.54	3.33	3.08
0.50	5.43	10.86	3.61	3.39	3.12
0.55	5.69	11.38	3.67	3.44	3.15
0.60	5.93	11.85	3.72	3.47	3.17
0.65	6.14	12.27	3.75	3.49	3.19
0.70	6.33	12.66	3.78	3.52	3.20
0.75	6.51	13.02	3.81	3.53	3.21
0.80	6.68	13.35	3.83	3.55	3.22
0.85	6.83	13.66	3.85	3.56	3.23
0.90	6.97	13.94	3.86	3.57	3.23
0.95	7.11	14.21	3.88	3.58	3.24
1.00	7.24	14.46	3.89	3.59	3.25
$C_{salt}=0.01$ M					
0.05	0.60	1.20	0.61	0.61	0.61
0.10	1.18	2.36	1.18	1.17	1.16
0.15	1.73	3.46	1.66	1.65	1.62
0.20	2.23	4.46	2.06	2.03	1.97
0.25	2.69	5.37	2.37	2.32	2.23
0.30	3.10	6.19	2.62	2.54	2.43
0.35	3.46	6.92	2.81	2.71	2.57
0.40	3.79	7.57	2.96	2.84	2.68
0.45	4.08	8.16	3.07	2.94	2.75
0.50	4.35	8.69	3.16	3.01	2.81
0.55	4.59	9.17	3.24	3.08	2.86
0.60	4.80	9.60	3.30	3.12	2.90
0.65	5.00	10.01	3.35	3.17	2.93
0.70	5.19	10.37	3.40	3.20	2.95
0.75	5.36	10.72	3.43	3.22	2.97
0.80	5.52	11.03	3.46	3.25	2.99
0.85	5.67	11.33	3.48	3.27	3.00
0.90	5.81	11.61	3.51	3.28	3.01
0.95	5.94	11.87	3.53	3.30	3.02
1.00	6.06	12.11	3.54	3.31	3.03
$C_{salt}=0.03$ M					
0.05	0.43	0.87	0.46	0.46	0.46
0.10	0.86	1.72	0.89	0.89	0.88
0.15	1.27	2.53	1.28	1.27	1.26
0.20	1.65	3.30	1.62	1.61	1.58
0.25	2.01	4.01	1.91	1.88	1.84
0.30	2.34	4.67	2.15	2.11	2.04
0.35	2.64	5.28	2.34	2.28	2.20
0.40	2.92	5.83	2.51	2.43	2.33
0.45	3.17	6.34	2.64	2.55	2.43
0.50	3.41	6.81	2.75	2.65	2.51
0.55	3.62	7.24	2.84	2.72	2.57
0.60	3.82	7.64	2.91	2.79	2.62
0.65	4.00	8.01	2.97	2.84	2.67
0.70	4.18	8.35	3.03	2.89	2.70
0.75	4.34	8.67	3.07	2.93	2.73
0.80	4.49	8.97	3.12	2.96	2.76
0.85	4.63	9.25	3.15	2.99	2.78
0.90	4.76	9.51	3.18	3.01	2.79
0.95	4.88	9.76	3.20	3.03	2.81
1.00	5.00	10.00	3.23	3.05	2.82
$C_{salt}=0.1$ M					
0.05	0.29	0.57	0.32	0.32	0.32
0.10	0.57	1.14	0.63	0.63	0.63
0.15	0.85	1.70	0.93	0.92	0.92
0.20	1.12	2.23	1.20	1.19	1.18
0.25	1.37	2.74	1.44	1.43	1.41
0.30	1.62	3.23	1.66	1.64	1.61
0.35	1.85	3.69	1.85	1.83	1.78
0.40	2.06	4.13	2.02	1.98	1.93
0.45	2.27	4.54	2.16	2.12	2.05
0.50	2.46	4.92	2.29	2.23	2.15
0.55	2.64	5.28	2.40	2.33	2.23
0.60	2.81	5.62	2.49	2.42	2.31
0.65	2.97	5.94	2.57	2.49	2.37
0.70	3.12	6.25	2.64	2.55	2.42
0.75	3.27	6.53	2.70	2.60	2.47
0.80	3.40	6.80	2.76	2.65	2.50
0.85	3.53	7.06	2.80	2.69	2.54
0.90	3.65	7.30	2.84	2.72	2.56
0.95	3.77	7.53	2.88	2.75	2.59
1.00	3.88	7.76	2.91	2.78	2.61

Charge $-\alpha e$ per DNA phosphate. Surface potential $y_0=-e\zeta/kT$. Mobilities $u_\parallel$ and $u_\perp$ in 10^{-4} cm^2 V^{-1} s^{-1}. Equivalent conductance [21,22] of counterions: $\lambda_{K^+}=73.5$, $\lambda_{TMA^+}=42.1$, $\lambda_{Tris^+}=29.7$; of coions: $\lambda_{Cl^-}=76.3$, $\lambda_{acetate^-}=40.9$.

coating the glass surfaces with a brushlike layer of an uncharged polymer such as polyacrylamide, used by Stellwagen et al. in capillary electrophoresis [16]. Such a precaution is strongly advised since the large variations among experimental results in important studies of electrophoretic stretch [13] and unhooking [15] of DNA near a gel/glass interface, suggest the influence of uncontrolled electroosmotic flow.

Table 2
Electrophoretic mobility, in 10^{-4} cm^2 V^{-1} s^{-1}, of DNA in 0.5×TBE buffer

$-e/$Å[a]	$-y_0$	$u_\parallel$	$u_\perp$	u_{av}
0.593	5.30	10.59	2.88	5.45
0.351	4.06	8.11	2.69	4.50
0.383[b]	4.27	8.53	2.74	4.67
0.226[b]	3.05	6.09	2.39	3.62
0.197[b]	2.75	5.50	2.26	3.34
0.320[c]	3.84	7.68	2.46	4.32
0.189[c]	2.66	5.33	2.21	3.25
0.132[c]	1.98	3.96	1.81	2.53
0.134	2.01	4.02	1.83	2.56

[a] Charge density.
[b] Estimate for staining with Ethidium bromide.
[c] Estimate for staining with TOTO-1.

We have treated the relaxation of DNA under free electrophoresis the same as relaxation of tethered DNA without a field. The reasonable agreement in Fig. 5 seems to validate the underlying assumption that elastic relaxation is the only process in both cases.

Acknowledgments

The author thanks Prof T.A.J. Duke for sharing the experimental data in Figs. 2 and 4 of Ref. [3].

Appendix A: Free solution electrophoresis of DNA[1]

We model 'kinetic' B-DNA as a cylinder with a hydrodynamic diameter of 20 Å, and a phosphate charge density of $-2/3.37 = -0.593$ e/Å, surrounded by a Poisson–Boltzmann atmosphere of small ions. Electrophoresis of the cylinder depends on its orientation. For long rods oriented parallel to the applied field, neglecting end effects, the mobility is given by von Smoluchowski's Equation, accounting for the backflow of the ionic atmosphere (electrophoretic effect),

$$u_\parallel = \frac{\varepsilon_0 D\zeta}{\eta} \tag{A1}$$

For rods oriented perpendicular to the external field, the mobility

$$u_\perp = g_\perp \frac{2\varepsilon_0 D\zeta}{3\eta} \tag{A2}$$

is lowered not only by the electrophoretic effect, but also by an asymmetry of the ionic atmosphere (relaxation effect) which decreases the applied field locally, depending on ionic mobilities and on ζ in a nonlinear fashion. The numerical factor $g_\perp$ in Eq. (A2) depends on properties of the cylinder and of the ionic medium. Some values are given in Ref. [8]. Table 1 lists for DNA at 25 °C, with a charge $-\alpha e$ per phosphate group, the dimensionless surface potential $y_0 = -e\zeta/kT$, and the mobilities $u_\parallel$ and $u_\perp$ in solutions of KCl, $N(CH_3)_4Cl$, (TMACl) and Tris–Acetate, as computed from the long rod theory [17,18]. Values of $g_\perp = 3u_\perp/2u_\parallel$ follow also from the data. The dependence of y_0 on the charge, and of $u_\perp$ on y_0 is strongly nonlinear. The difference between $u_\parallel$ and $u_\perp$ shows the large effect of the orientation of the cylinder. The dependence of $u_\perp$ on ion type through the relaxation effect is substantial, in particular at high potential and low ionic strength. The random average mobility

$$u_{av} = \frac{1}{3}u_\parallel + \frac{2}{3}u_\perp \tag{A3}$$

is observed in free solution electrophoresis of DNA.

We now discuss some data relevant to gel electrophoresis of DNA and related experiments. Using capillary electrophoresis, Stellwagen et al. [16] measured the free solution mobility of DNA fragments of various sizes at 25 °C in buffer solution of 0.04 M Tris–Acetate and 0.001 M EDTA, pH 8.0. For fragments longer than approximately 400 base pairs (bp) the mobility was constant at $u_{av} = 3.75\times10^{-4}$ cm^2 V^{-1} s^{-1}. At pH 8 about half of the Tris–base is ionized, and neutralized by acetic acid. Neglecting the presence of EDTA, we assume that the ionic strength of the buffer solution is 0.02 M. For this solution the long rod theory [17,18] gives $\alpha = 0.39$, suggesting that more than half of the $Tris^+$ counterions are inside the shear surface of the DNA. We compare this with the classic study by Ross and Scruggs

[1] Upon request the author will email his FORTRAN program for electrophoresis [18] to interested readers.

Table 3
Effects of kinetic diameter of B-DNA on its electrophoresis in TMACl solutions

Diameter (Å)	M_{TMACl}	y_0	$u_{\parallel}$	$u_{\perp}$	u_{av}
B-DNA, charge density -0.593 e/Å					
20	0.002	7.63	15.26	3.68	7.54
20	0.005	6.73	13.46	3.48	6.80
20	0.010	6.06	12.11	3.31	6.25
20	0.020	5.39	10.77	3.14	5.69
20	0.050	4.52	9.03	2.93	4.97
20	0.100	3.88	7.75	2.78	4.44
22	0.002	7.44	14.88	3.64	7.39
22	0.005	6.55	13.09	3.43	6.65
22	0.010	5.87	11.74	3.27	6.09
22	0.020	5.21	10.41	3.10	5.53
22	0.050	4.34	8.68	2.89	4.82
22	0.100	3.70	7.41	2.74	4.30
24	0.002	7.27	14.54	3.60	7.25
24	0.005	6.38	12.75	3.39	6.51
24	0.010	5.70	11.41	3.22	5.95
24	0.020	5.04	10.08	3.06	5.40
24	0.050	4.18	8.35	2.85	4.69
24	0.100	3.55	7.09	2.71	4.17
Stained-DNA, charge density -0.383 e/Å					
20	0.002	6.51	13.01	3.60	6.73
20	0.005	5.64	11.27	3.35	5.99
20	0.010	4.99	9.97	3.16	5.43
20	0.020	4.35	8.70	2.96	4.87
20	0.050	3.54	7.08	2.69	4.15
20	0.100	2.96	5.91	2.48	3.63
22	0.002	6.32	12.64	3.55	6.58
22	0.005	5.46	10.91	3.31	5.84
22	0.010	4.81	9.62	3.11	5.28
22	0.020	4.18	8.36	2.90	4.72
22	0.050	3.38	6.75	2.63	4.00
22	0.100	2.80	5.61	2.42	3.48
24	0.002	6.16	12.31	3.52	6.45
24	0.005	5.29	10.58	3.25	5.70
24	0.010	4.65	9.30	3.06	5.14
24	0.020	4.02	8.04	2.85	4.58
24	0.050	3.23	6.46	2.58	3.87
24	0.100	2.67	5.33	2.37	3.36

Surface potential $y_0 = -e\zeta/kT$. Mobilities $u_{\parallel}$, $u_{\perp}$, and u_{av} in 10^{-4} cm^2 V^{-1} s^{-1}. Equivalent conductance: $\lambda_{TMA^+} = 42.1$, $\lambda_{Cl^-} = 76.3$.

[19] who measured electrophoresis of calf thymus DNA in various salt solutions at 1.3 °C, using the Tiselius moving boundary method. As shown earlier [17], their results in 0.05–0.6 M solutions of TMACl lead to DNA surface charges corresponding to approximately $\alpha = 1$. The difference between $\alpha = 0.39$ in Tris–Acetate and $\alpha = 1$ in TMACl is at least partly of electrostatic origin, due to the location of the charge in the cations. In $Tris^+$ the N^+ charge is at the outside of the ion, giving a high local positive potential for binding to the negative DNA surface, in addition to the possibility of hydrogen bonding with the OH groups of Tris. On the other hand, in TMA^+ the N^+ charge is in the center of the ion, giving a much smaller potential for local binding to DNA, and no hydrogen bonding with the DNA surface.

Gel electrophoresis of DNA is often carried out in 0.045 M Tris–Borate + 1 mM EDTA buffer (0.5×TBE). Stellwagen et al. [16] found in this buffer $u_{av} = 4.5 \times 10^{-4}$ cm^2 V^{-1} s^{-1} for the free solution mobility of DNA fragments larger than 400 bp. Taking an ionic strength of 0.022 M (correcting the previously used value [1] of 0.01 M), and assuming the same equivalent conductance of Borate as of Acetate, this mobility corresponds to a DNA charge of $\alpha = 0.59$. Compared with $\alpha = 0.39$ for DNA in Tris–Acetate buffer, the replacement of Acetate by Borate ions makes DNA substantially more negative.

As in Ref. [3], single molecule experiments related to gel electrophoresis are often carried out by fluorescent microscopy of DNA stained with an intercalating dye. In general, the charge of the stained DNA is uncertain because there are no suitable electrophoretic experiments. Here we derive some estimates for DNA in 0.5×TBE buffer, stained with Ethidium bromide, a much used monovalent, monointercalating dye. At a typical dye concentration of 0.5 μg ml^{-1} intercalation of Ethidium bromide increases the contour length of DNA by 31% [20]. We assume a rise of 3.37 Å per bp and the same per intercalating dye molecule. Then the intrinsic linear charge density of unstained DNA, $-2/3.37 = -0.593$ e/Å, changes to $-(2-0.31)/(3.37 \times 1.31) = -0.383$ e/Å for the stained DNA. It is likely that stained DNA interacts with bufferions in much the same way as unstained DNA, that is, giving a charge reduction of approximately 41%, see above. In stained DNA we can apply this reduction to the net charge, giving a linear charge density of $-0.59 \times (2-0.31)/(3.37 \times 1.31) = -0.226$ e/Å, or

reduce just the phosphate charge by 41%, giving $-(0.59\times2-0.31)/(3.37\times1.31)=-0.197\ e/\text{Å}$.

Bakajin et al. [3] stained T4 DNA with TOTO-1, a bis-intercalating dye with four positive charges per molecule. With a 30% increase in contour length, the intrinsic charge of the stained DNA is $-(2-2\times0.30)/(3.37\times1.30)=-0.320\ e/\text{Å}$. Assuming the same interaction with buffer as above, the net charge density becomes $-0.59(2-2\times0.30)/(3.37\times1.30)=-0.189\ e/\text{Å}$ or $-(0.59\times2-2\times0.30)/(3.37\times1.30)=-0.132\ e/\text{Å}$. Table 2 gives the ζ potentials and the electrophoretic mobilities of DNA with the charge densities derived above.

The results in Table 1 and 2 depend significantly on the value assumed for the kinetic diameter of DNA, $d=20$ Å in this paper. Actually, this value is rather uncertain. An associated problem is using the same shear surface for interpreting electrophoresis and friction experiments. Earlier computations were based on different kinetic diameters, $d=24$ Å [1,8,17] and $d=22$ Å [2]. Suitable experiments on DNA with a known electrophoretic charge density could be used to determine the kinetic diameter of DNA more accurately. The electrophoretic experiments by Ross and Scruggs [19,23] on DNA in various ionic solutions suggest strongly that TMA^+ counterions do not interact specifically with B-DNA. So in solutions of TMACl one expects that the electrophoretic charge of DNA equals its intrinsic phosphate charge with linear charge density $-2/3.37=-0.593\ e/\text{Å}$. For DNA stained with Ethidium bromide, 0.5 $\mu g\,ml^{-1}$, a reasonable estimate of the intrinsic charge density is $-0.383\ e/\text{Å}$, see above. For these cases Table 3 gives the predicted electrophoretic mobilities for DNA cylinders with diameters $d=20$, 22, and 24 Å as a function of TMACl concentration.

References

[1] D. Stigter, C. Bustamante, Theory for the hydrodynamic and electrophoretic stretch of tethered B-DNA, Biophys. J. 75 (1998) 1197–1210.

[2] D. Stigter, Influence of agarose gel on electrophoretic stretch, on trapping, and on relaxation of DNA, Macromolecules 33 (2000) 8878–8889.

[3] O.B. Bakajin, T.A.J. Duke, C.F. Chou, S.S. Chan, R.H. Austin, E.C. Cox, Electrohydrodynamic stretching of DNA in confined environments, Phys. Rev. Let. 80 (1998) 2737–2740.

[4] J. Happel, H. Brenner, Low Reynolds Number Hydrodynamics, Prentice Hall, Englewood Cliffs, NJ, 1965.

[5] A. Oberbeck, Ueber stationäre Flüssigkeitbewegungen mit Berücksichtigung der inneren Reibung, Crelles. J. 81 (1876) 62–80.

[6] W. Eimer, R. Pecora, Rotational and translational diffusion of short rodlike molecules in solution: oligonucleotides, J. Chem. Phys. 94 (1991) 2324–2329.

[7] B.H. Zimm, Extension in flow of a DNA molecule tethered at one end, Macromolecules 31 (1998) 6089–6098.

[8] D. Stigter, Shielding effects of small ions in gel electrophoresis of DNA, Biopolymers 31 (1991) 169–176.

[9] J.F. Marko, E.D. Siggia, Stretching DNA, Macromolecules 28 (1995) 8759–8770.

[10] T.L. Hill, An Introduction to Statistical Thermodynamics, Addison-Wesley, Reading, MA, 1960, Chapter 13.

[11] C. Bouchiat, M.D. Wang, J.F. Allemand, T. Strick, S.M. Block, V. Croquette, Estimating the persistence length of a worm-like chain molecule from force-extension measurements, Biophys. J. 76 (1999) 409–413.

[12] C. Rivetti, M. Guthold, C. Bustamante, Scanning force microscopy of DNA deposited onto mica: equilibrium versus kinetic trapping studied by statistical polymer chain analysis, J. Mol. Biol. 264 (1996) 919–932.

[13] S.B. Smith, A.J. Bendich, Electrophoretic charge density and persistence length of DNA as measured by fluorescence microscopy, Biopolymers 29 (1990) 1167–1173.

[14] S. Gurrieri, S.B. Smith, C. Bustamante, Trapping of megabase-sized DNA molecules during agarose gel electrophoresis, Proc. Natl. Acad. USA 96 (1999) 453–458.

[15] L. Song, M. Maestre, Unhooking of U-shaped DNA molecule undergoing gel electrophoresis, J. Biomol. Struct. Dynamics 9 (1991) 87–99, The extension-time curves in this paper of the two legs of the U during unhooking can be extrapolated back to equal extension of both legs. This gives the electrophoretic stretch of the stationary molecules, unaffected by any contact friction with the gel. For five T4 DNA molecules in 4 V/cm these equilibrium extensions range from about 21 to 40 μm, less than estimated for electrophoretic stretch in the gel or in gel-free buffer. This strongly suggests the presence of significant electroosmotic flow in a nonuniform gel medium.

[16] N.C. Stellwagen, C. Gelfi, P.G. Righetti, The free solution mobility of DNA, Biopolymers 42 (1997) 687–703.

[17] J.A. Schellman, D. Stigter, Electrical double layer, zeta potential, and electrophoretic charge of double-stranded DNA, Biopolymers 16 (1977) 1415–1434.

[18] D. Stigter, Electrophoresis of highly charged colloidal cylinders in univalent salt solutions. I. Mobility in transverse field, J. Phys. Chem. 82 (1978) 1417–1423.
[19] P.D. Ross, R.L. Scruggs, Electrophoresis of DNA. III. The effect of several univalent electrolytes on the mobility of DNA, Biopolymers 2 (1964) 231–236.
[20] S.B. Smith, L. Finzi, C. Bustamante, Direct mechanical measurements of the elasticity of single DNA molecules by using magnetic beads, Science 258 (1992) 1122–1126.
[21] R.A. Robinson, R.H. Stokes, Electrolyte Solutions, second ed., Butterworths, London, 1970.
[22] S.D. Klein, R.G. Bates, Conductance of Tris(hydroxymethyl)-aminomethane hydrochloride (Tris–HCI) in water at 25 and 37 °C, J. Solution Chem. 9 (1980) 289–292.
[23] P.D. Ross, R.L. Scruggs, Electrophoresis of DNA. II. Specific interactions of univalent and divalent cations with DNA, Biopolymers 2 (1964) 79–89.